Characterization of Redlen high-flux CZT on MM-PAD detectors

Lena Franklin

laf233@cornell.edu

Cornell University

January 2026

Line-pair mask radiograph using HF-CZT sensor

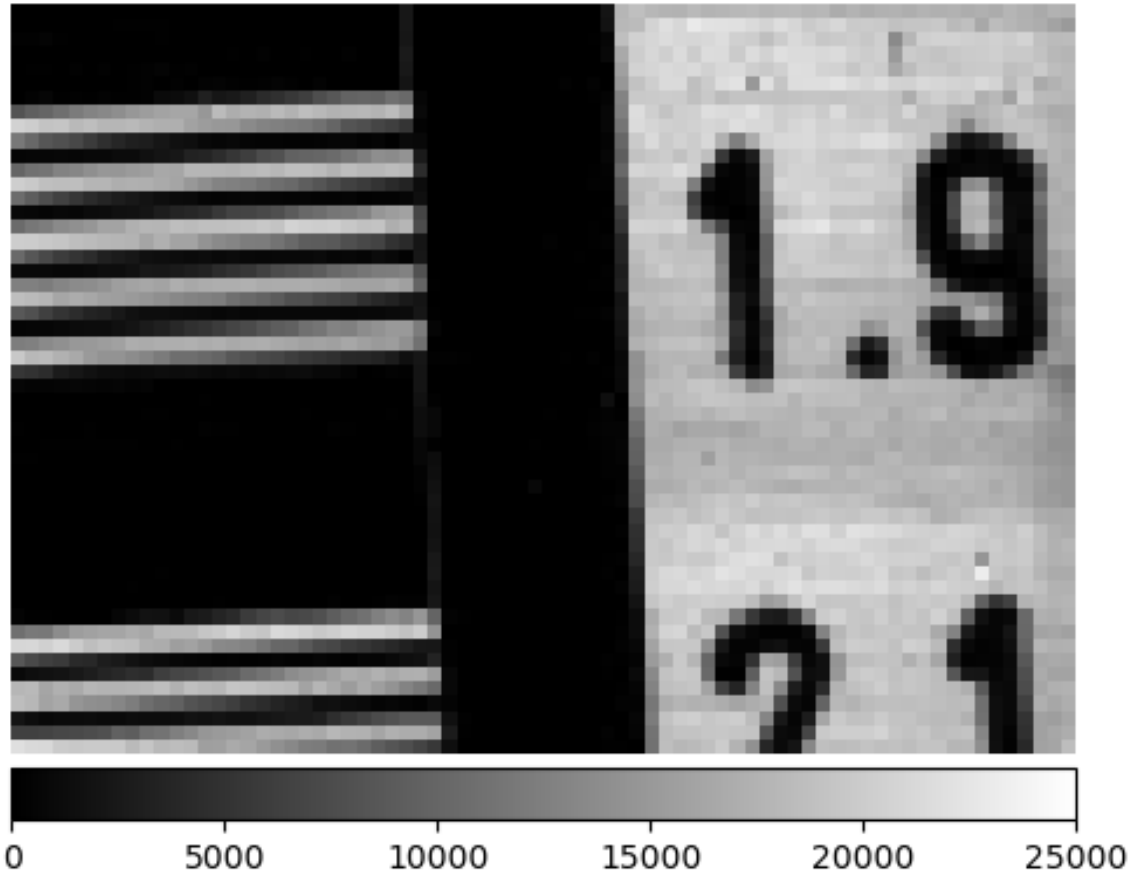

Thom-Gruner Group


Julia Thom-Levy
Physics faculty


Sol Gruner,
Emeritus faculty


Mark Tate,
Staff Scientist


Lena Franklin,
Graduate student


Nick Brown,
ASIC designer

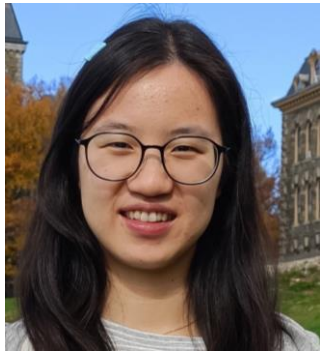
Sixuan Li
Graduate student


Marianne Hromalik, ECE
faculty SUNY Oswego

Collaborators on High-Z sensor materials and other projects:

Shanks (CHESS)
Rumaiz, Carini, Siddons, Capocasa (BNL)
Miceli (ANL),
Segal, Kenney (SLAC), Leitz (MIT LL)
Muller Group (Cornell)

Group ASICs:

- MM-PAD 1
- MM-PAD 2
- Keck-PAD

High-speed, high-energy X-ray diffraction

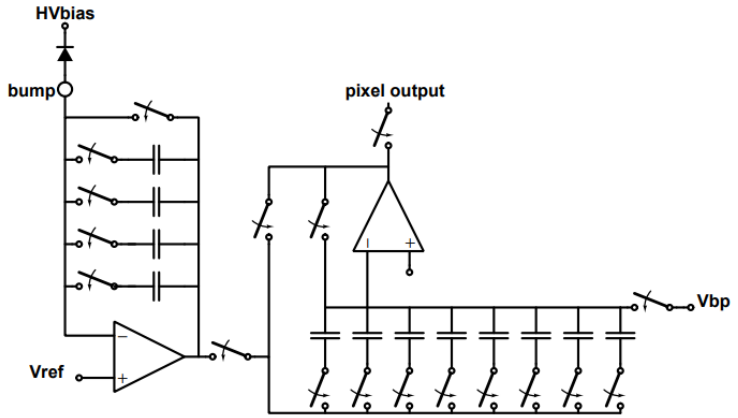

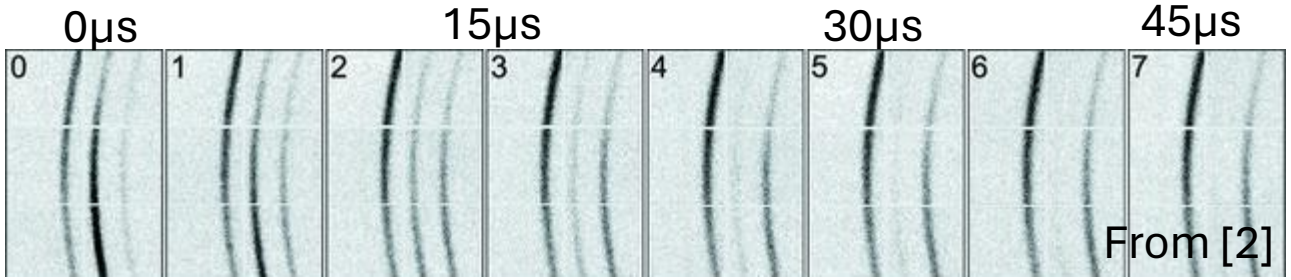

From [2]

New 77 ns 16 frame burst-rate detector is currently being designed for use at Advanced Photon Source (APS)

STEM (electron ptychography

with David Muller's group

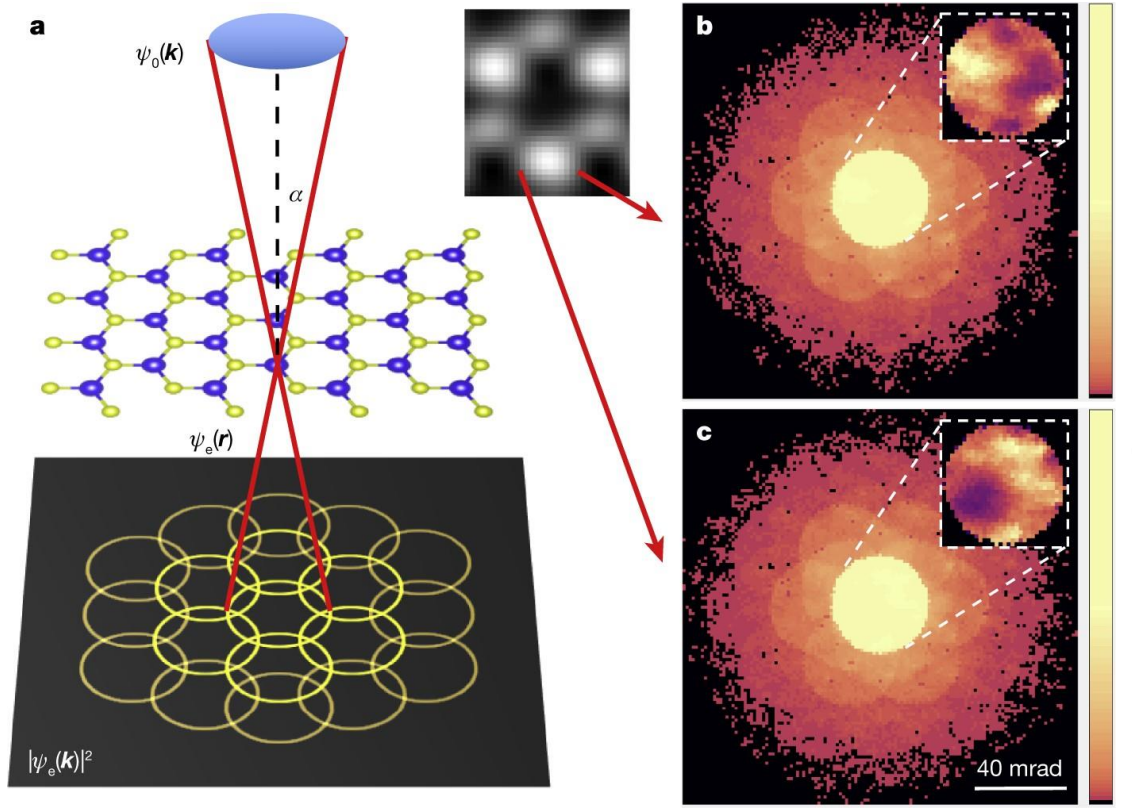

From [3]

Both require: high QE, polarization resistance, fast response (fast CC and limited afterglow)

Redlen high-flux CZT

- Improve resistance to polarization (compared to standard CZT, CdTe) by improving hole transport
- 2 mm thick sensor with Pt contacts, Schottky behavior due to Te and Cd rich faces
- Bonded to two ASICs developed at Cornell, MM-PAD 1 and MM-PAD 2

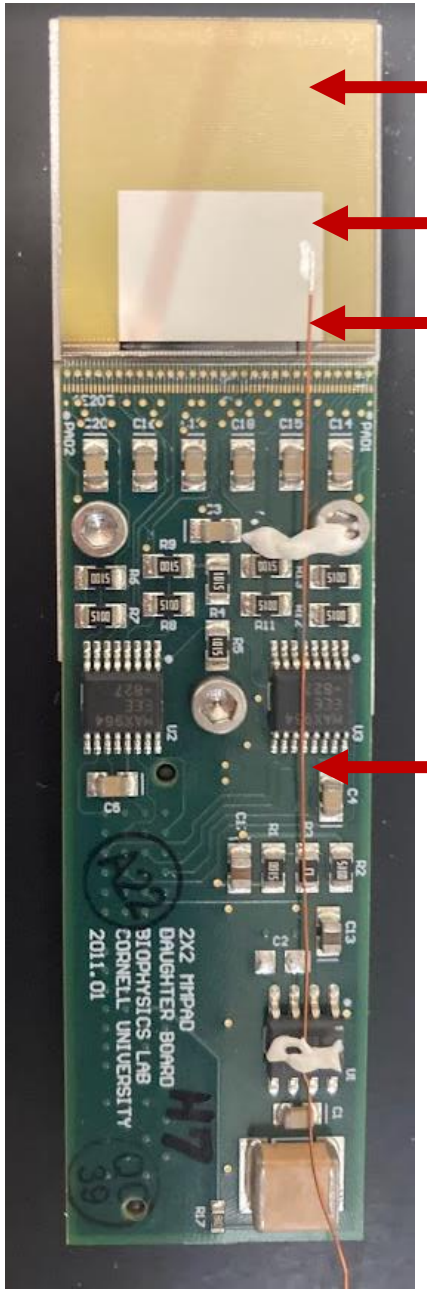

CZT sensor bonded to MM-PAD ASIC

MM-PAD ASICs

- Charge integrating, previously bonded to Si, CdTe, Ge…
- Combined analog-digital readout
- Used in both X-ray and electron sensing applications
  - Deformation of metals/residual stress measurements
  - Electron ptychography

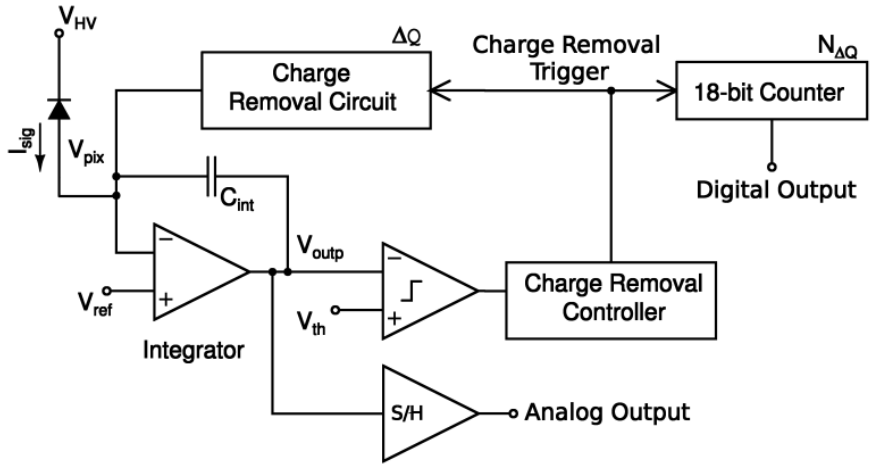

	MM-PAD-1 (8 keV equivalent)	MM-PAD-2.1 (20 keV equivalent)
Format	128×128	128×128
Pixel pitch	150 µm	150 µm
Sensor	Si,CdTe	Si,CdTe
Charge Collection	holes only	electrons or holes
Frame rate (FR)	1.1 kHz	10 kHz
Duty Cycle, max FR	0%	99%
Read noise	0.16 photon	0.13 photon
Well capacity	4.7×10^7 photons	2.2×10^7 photons
Instantaneous count rate	$> 10^{12}$ ph/pix/s	$> 10^{12}$ ph/pix/s

Sensor gain – electron collecting sensor

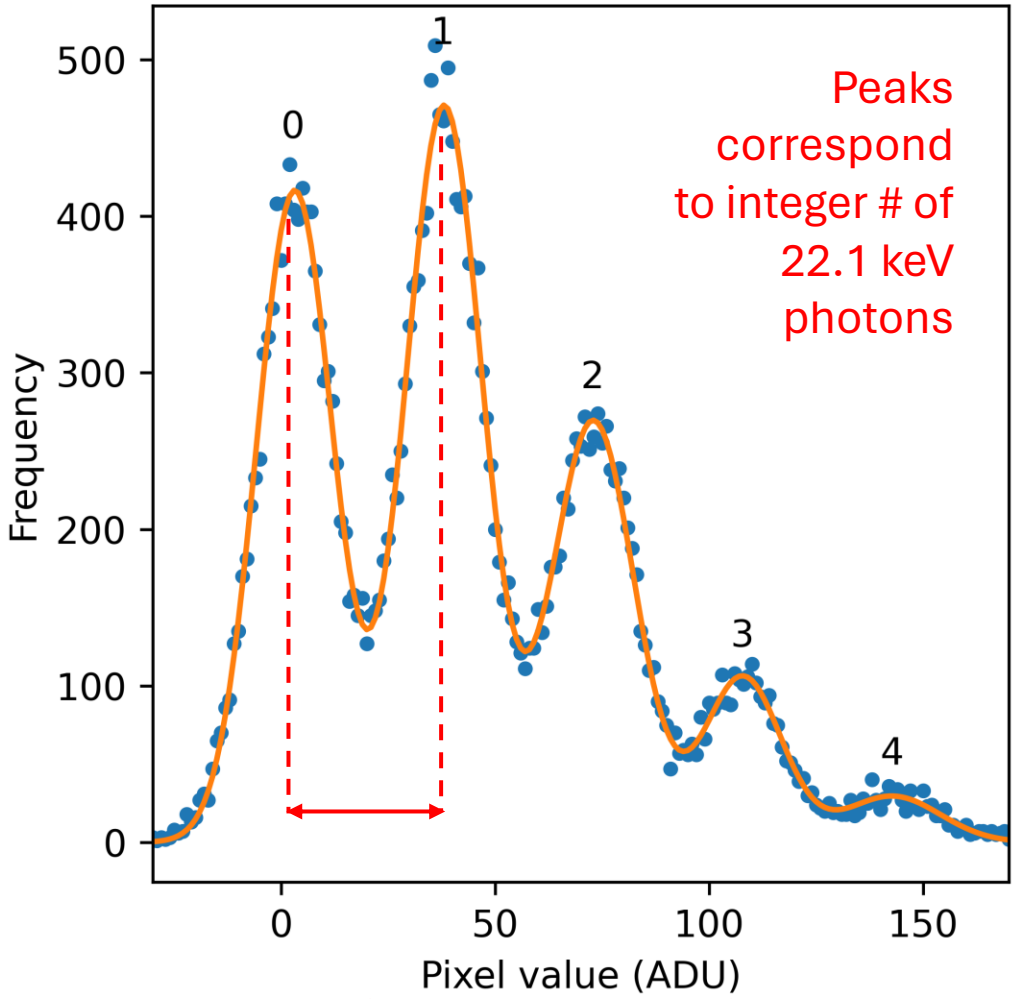

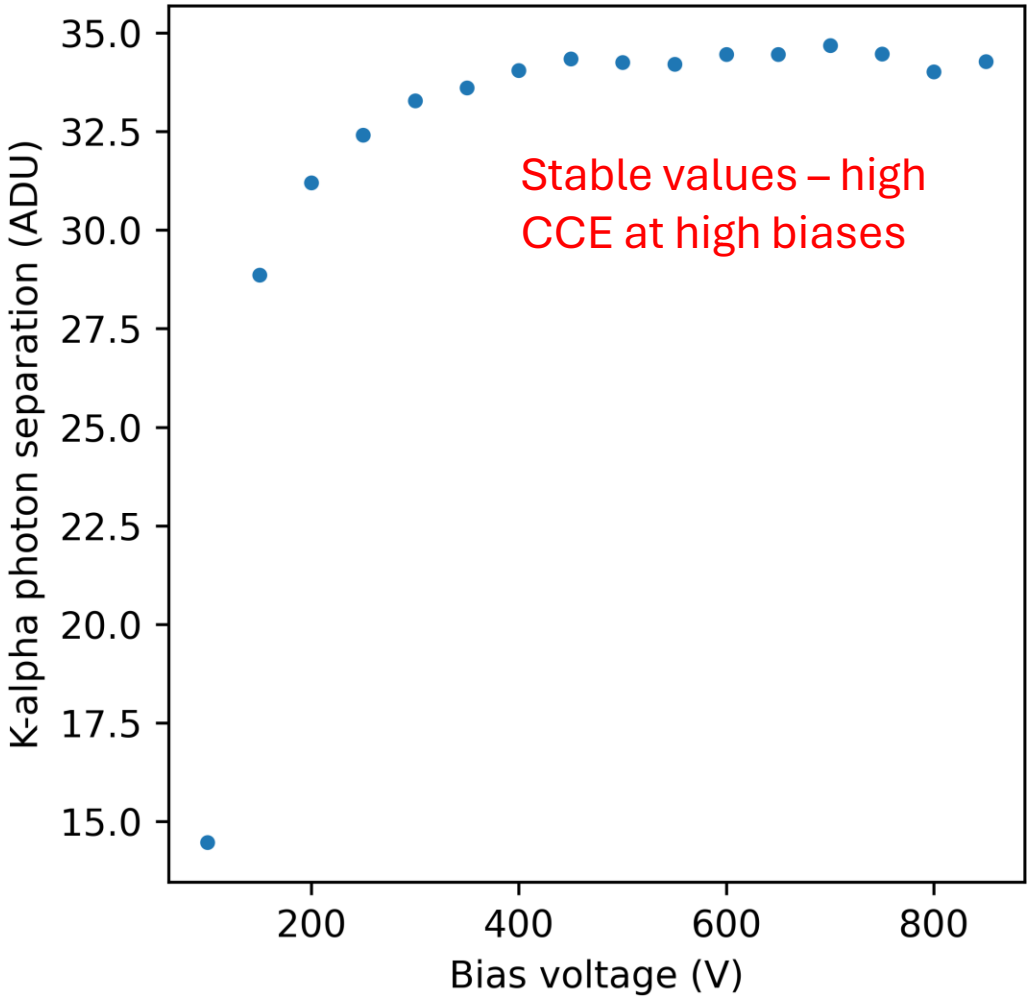

Fit to sum of gaussians

Sensor gain computed from peak separation

Charge Collection Efficiency

Hole collecting

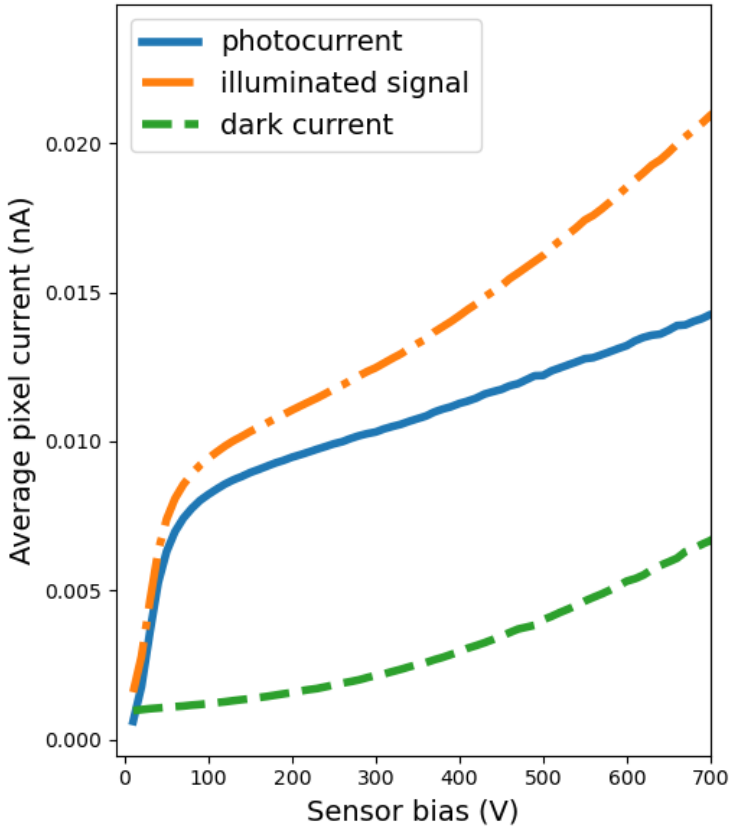

Electron collecting

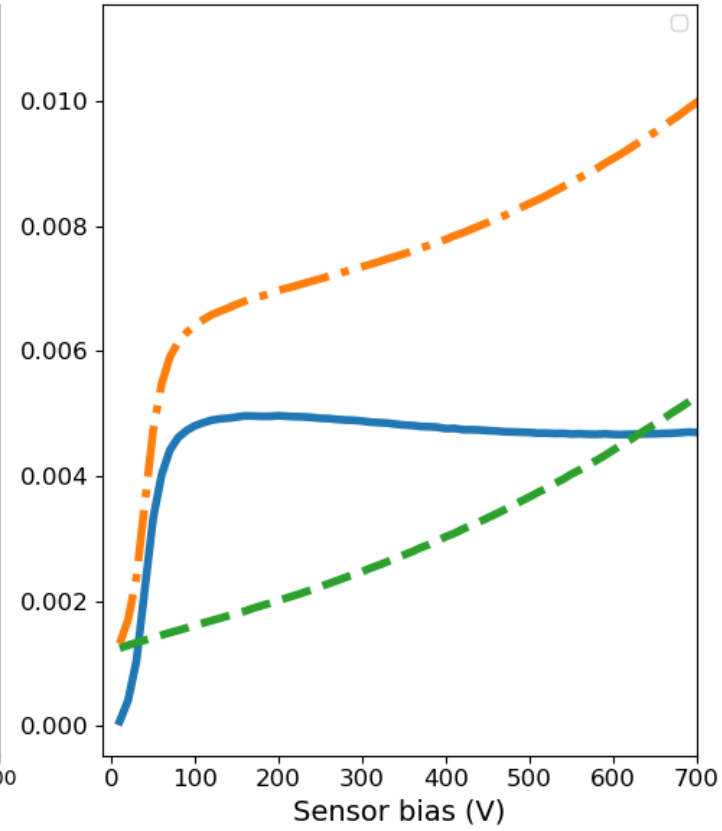

Theory

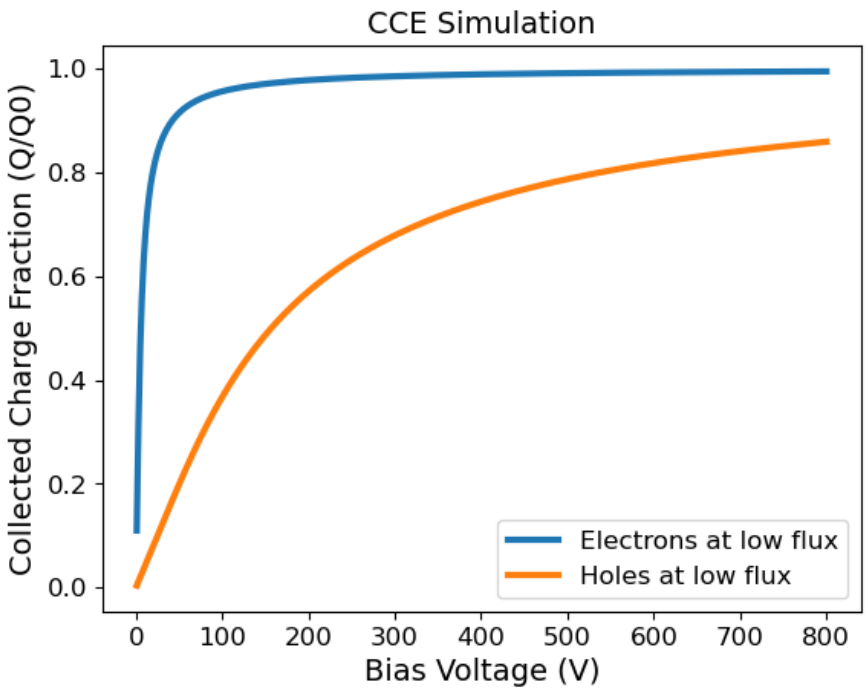

At typical biases of 500 – 1000 V, e- collecting configuration offers significantly better CCE.

Spatial Resolution

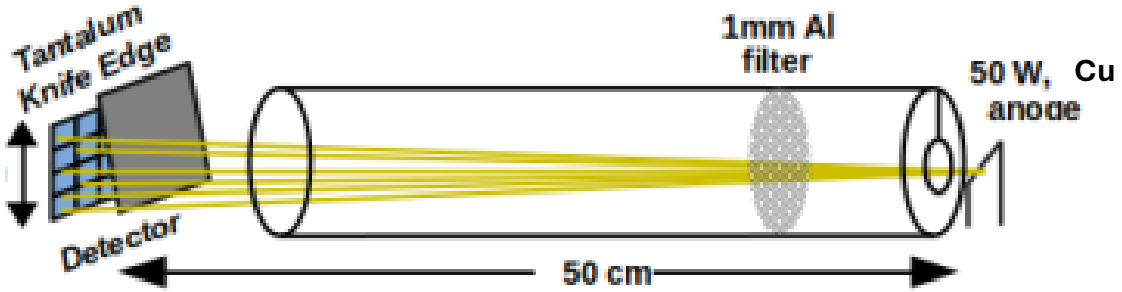

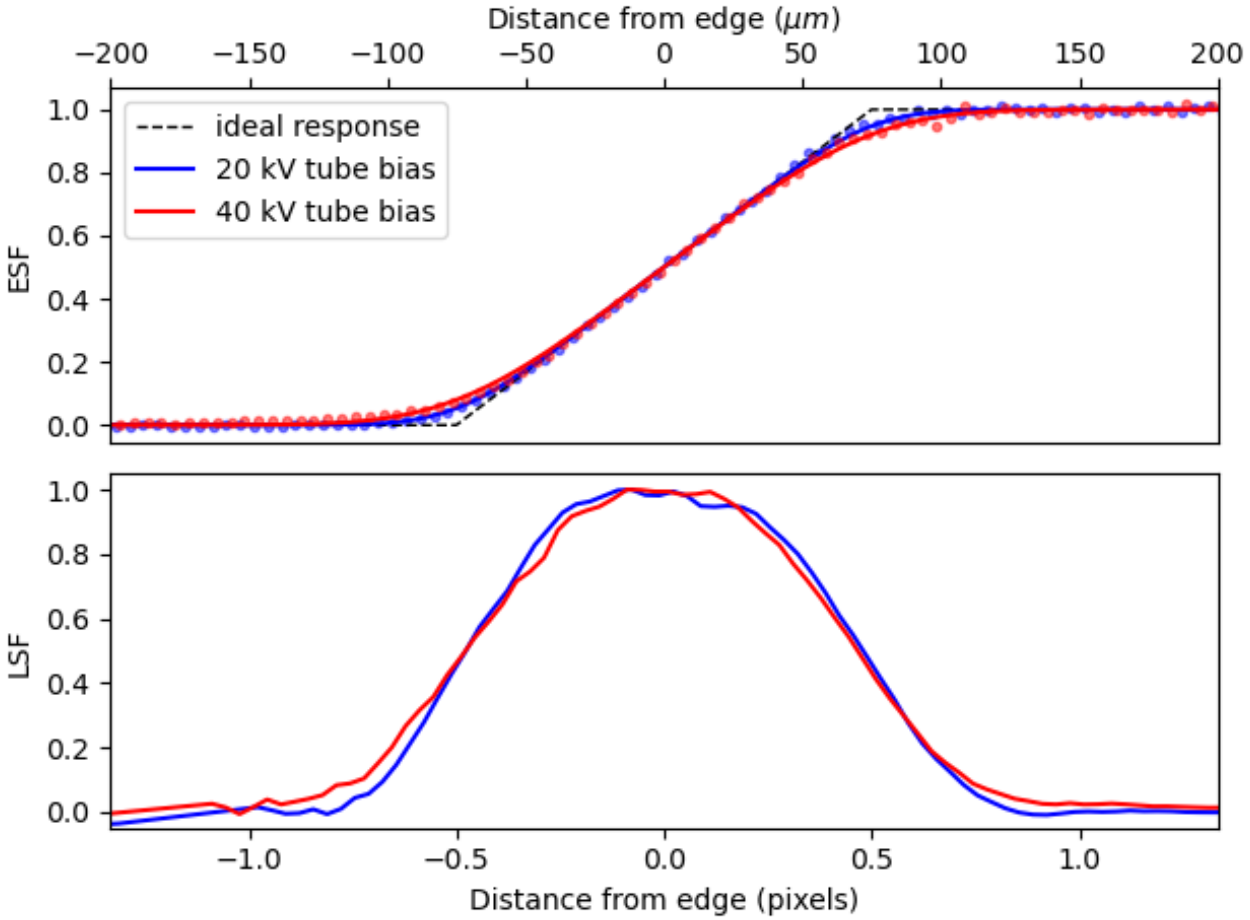

Gaussian standard deviation:

20 kV tube bias: 20 μm

Below Cd and Te fluorescence edge

40 kV tube bias + 1mm Al filter: 30 μm

Fluorescence within sensor broadens CC

Electron collecting, 700 V bias

Polarization – Preliminary Results

- Preliminary: only conducted with in-lab source which provides no more than 10^9 ph/mm^2/s
- Some change in total spot intensity at high fluxes of low-energy (<20 keV) X-rays
- Improvement over CdTe (at same E-field)

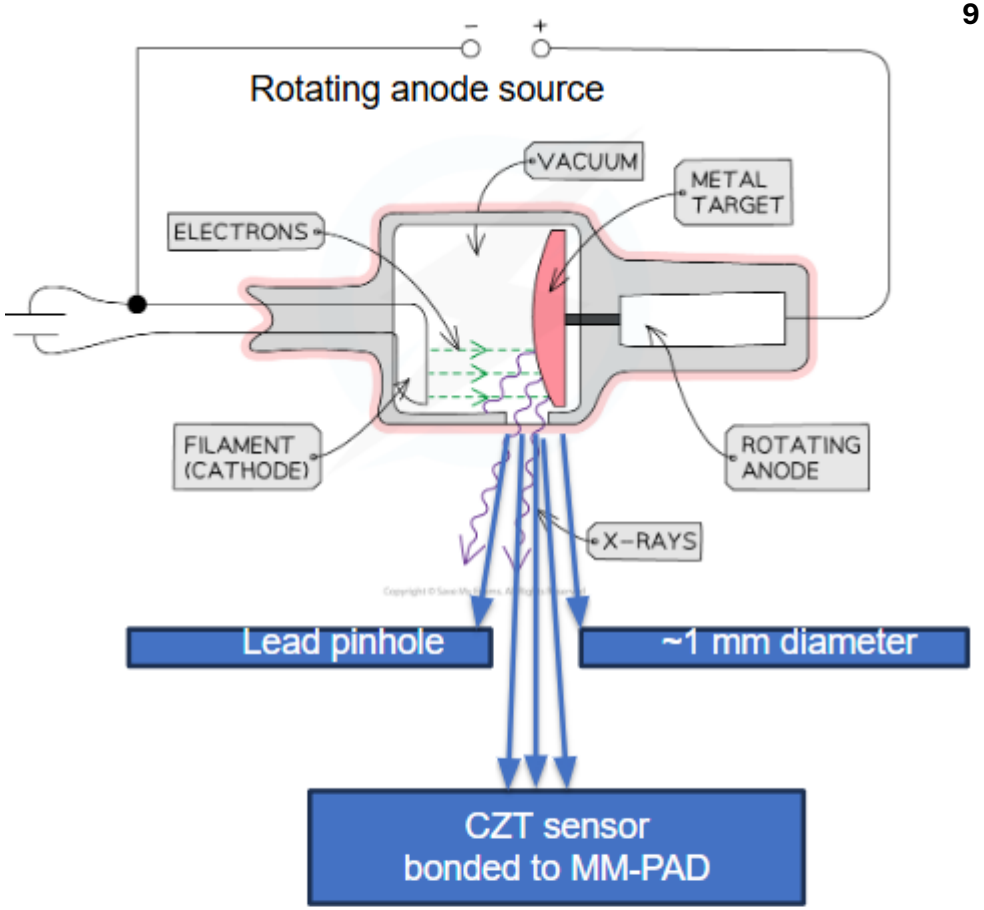

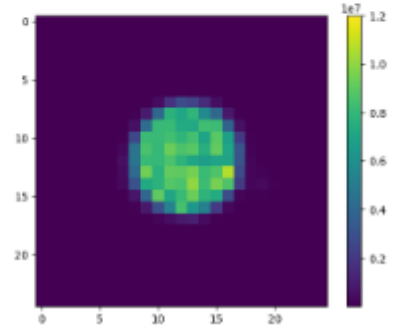

Beam spot on MM-PAD detector

Low energy X-ray polarization

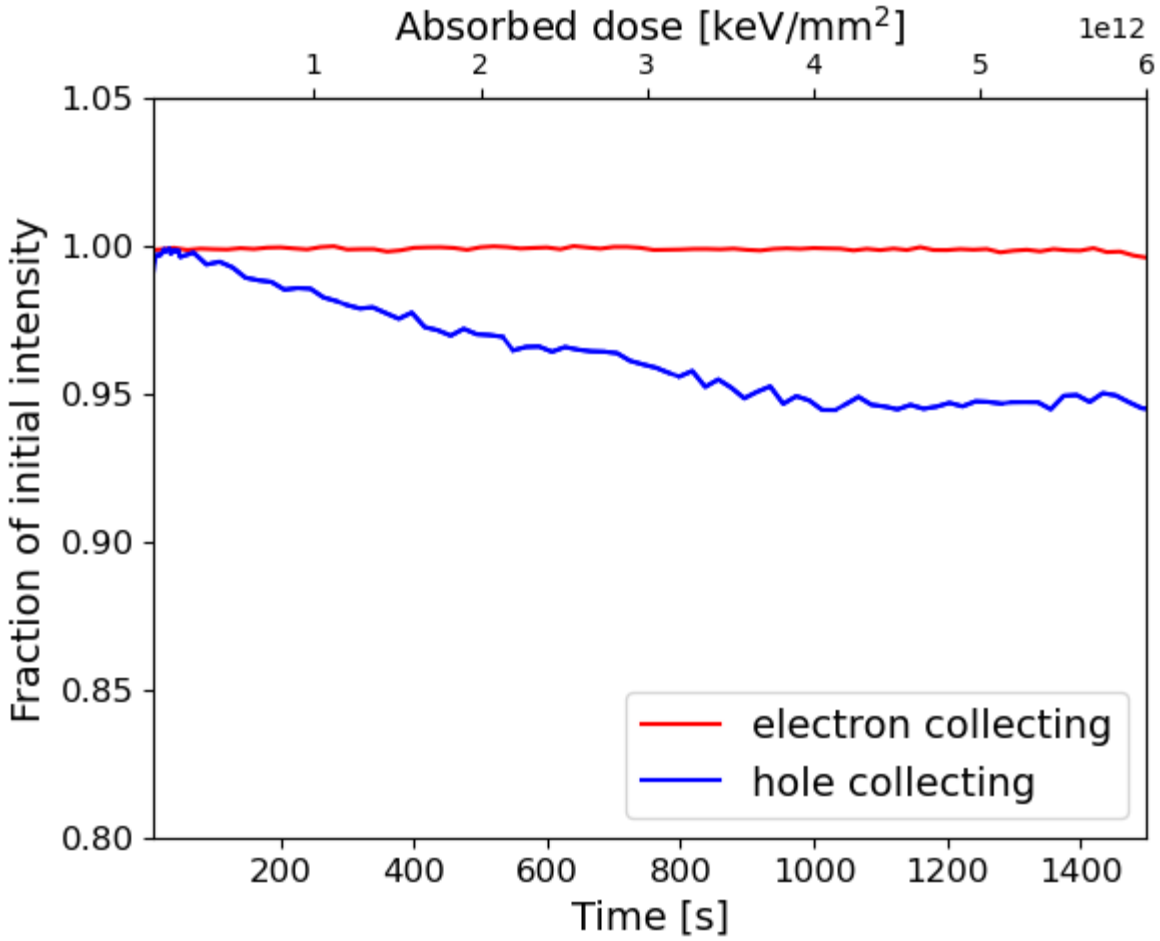

- Broad spectrum <20 keV photons (Cu source, Kalpha ~8 keV)
- **At low X-ray energies, hole-collecting HF-CZT shows modest reduction in signal after ~10^{12} keV/mm²/s total dose**

Effects of increasing x-ray energy

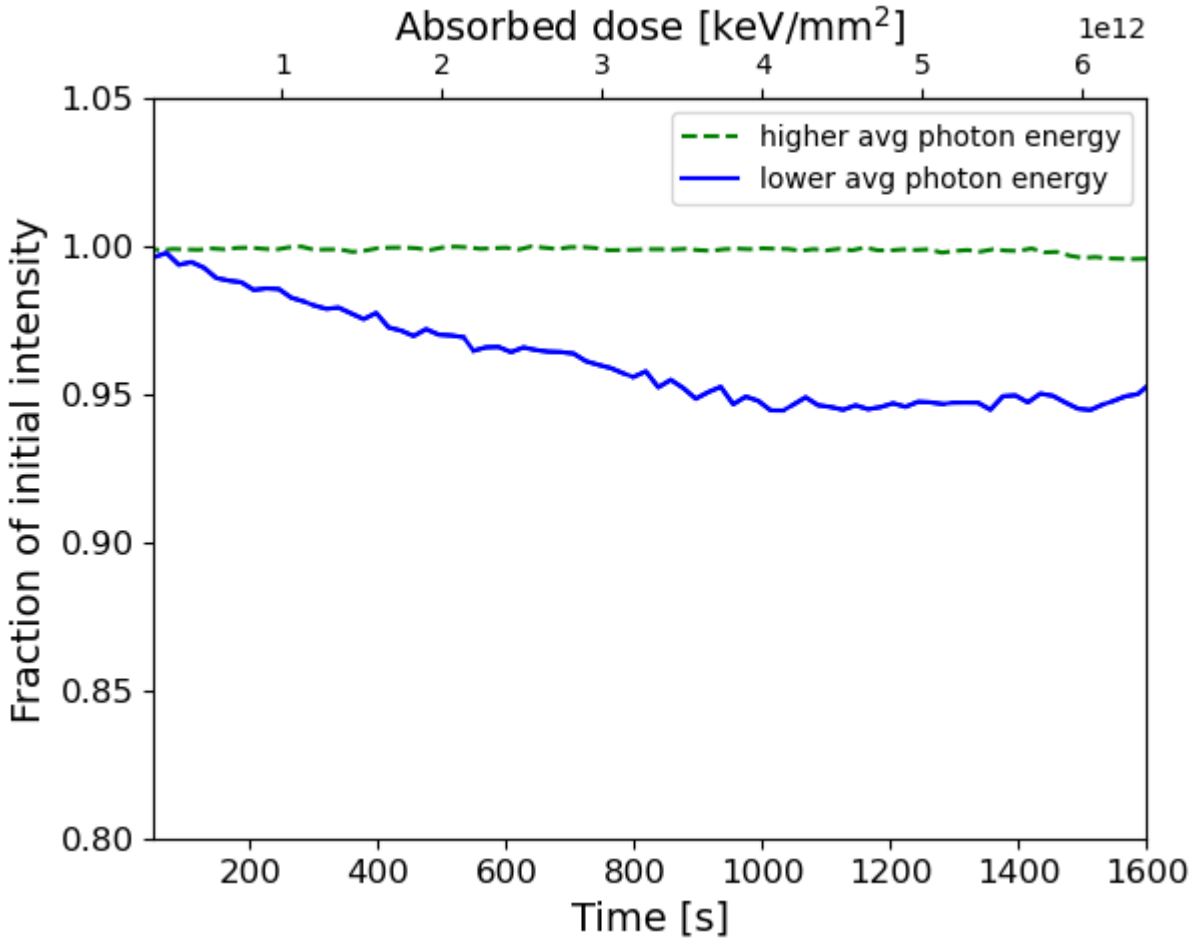

- Higher average photon energy: 30 keV tube bias, 0.2 mm Al attenuation
- Lower average photon energy: 20 keV tube bias, 0.01 mm Al attenuation
- **Filter low energy photons to prevent polarization**

Polarization response: comparison with CdTe

Comparison: hole-collecting HF-CZT and hole-collecting CdTe at 275 V/mm bias

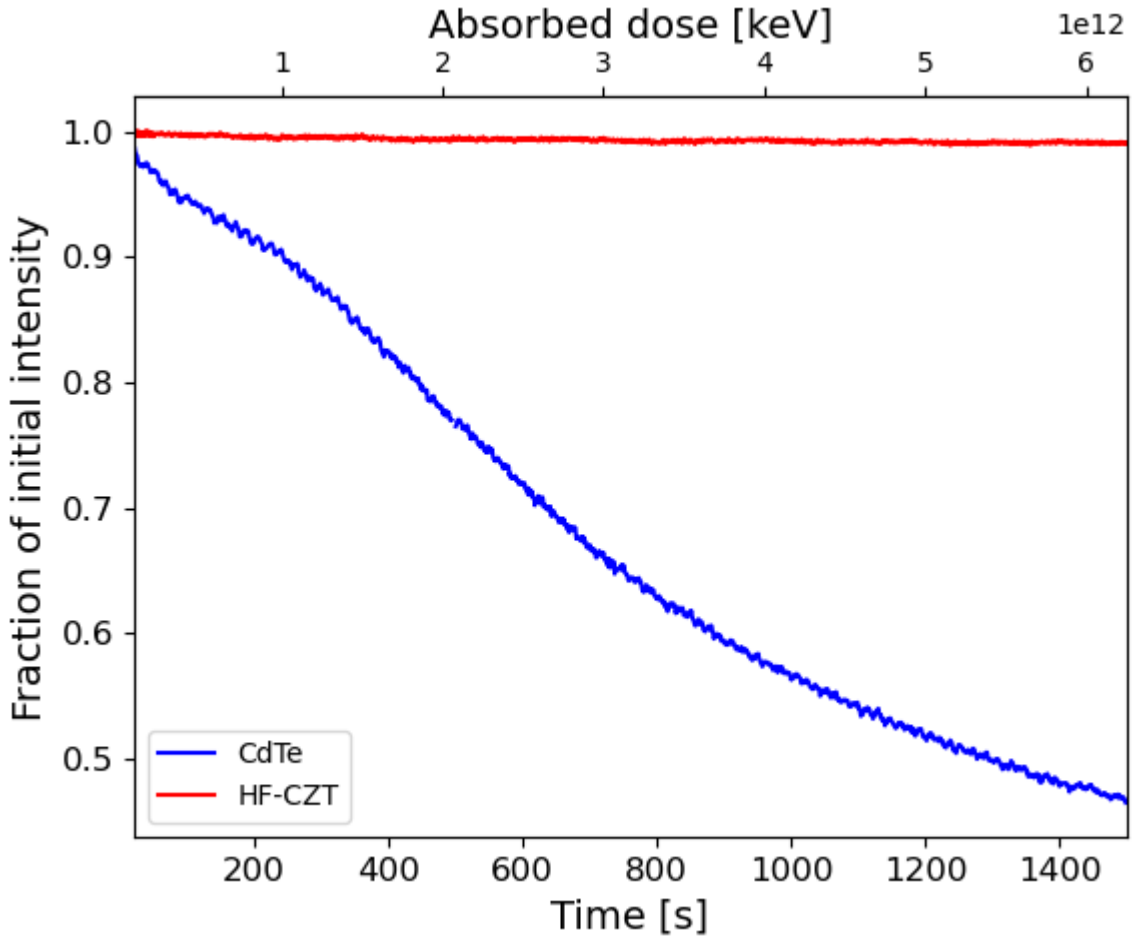

- 2 mm thick HF-CZT, 750 um thick CdTe
- 30 keV tube bias, 0.2 mm Al attenuation
- **HF-CZT shows improved polarization resistance for higher energy photons, and improved polarization resistance compared to CdTe**

Changes in spot shape

- Spot shape changes slightly as dose is absorbed, even if total spot intensity doesn't change
- Electron collecting spot shrinks slightly, hole-collecting spot grows slightly

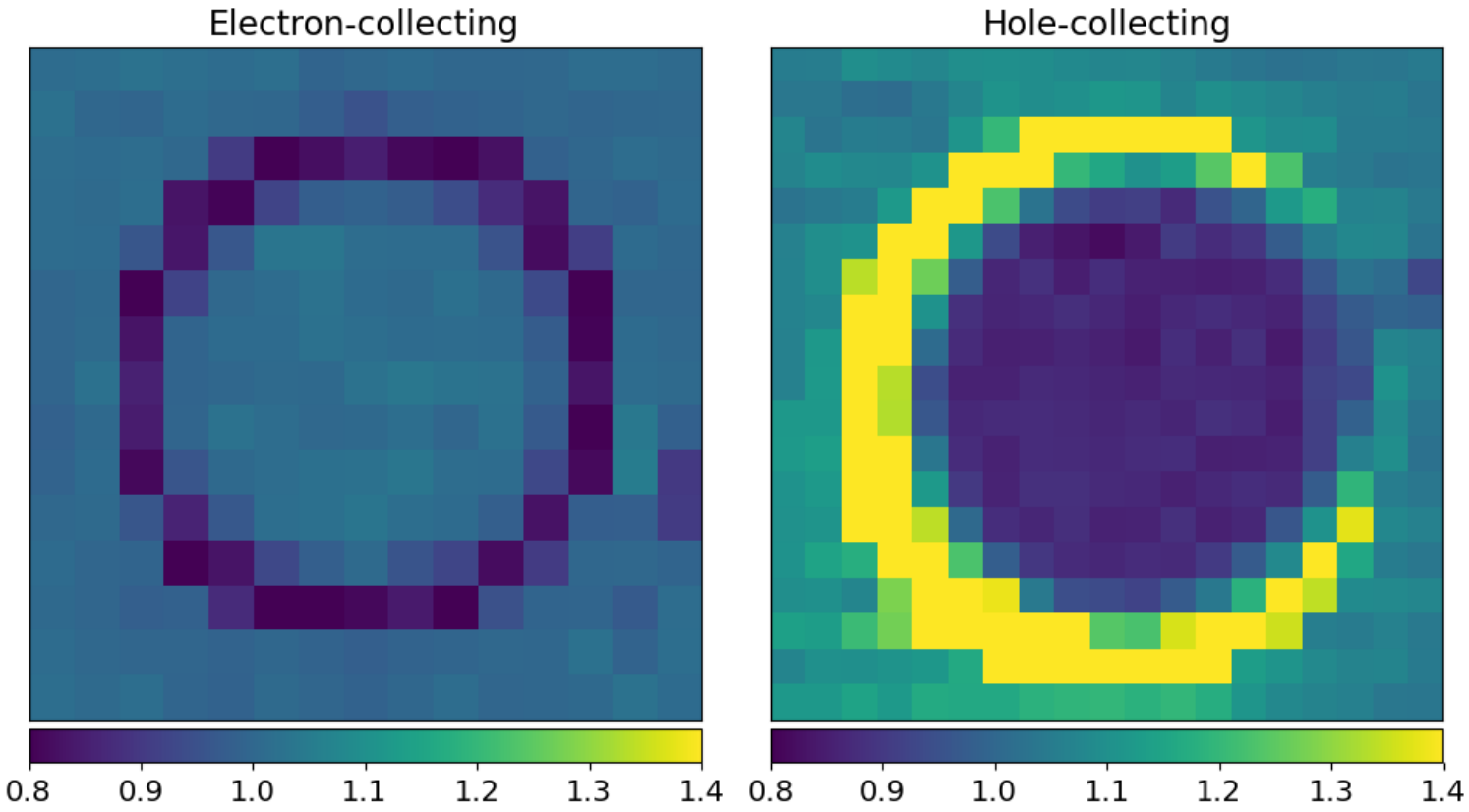

Image of the spot before polarization divided by the image of the spot after polarization

Afterglow

- Significant afterglow observed at low to moderate fluxes
- Afterglow magnitude increases with applied bias

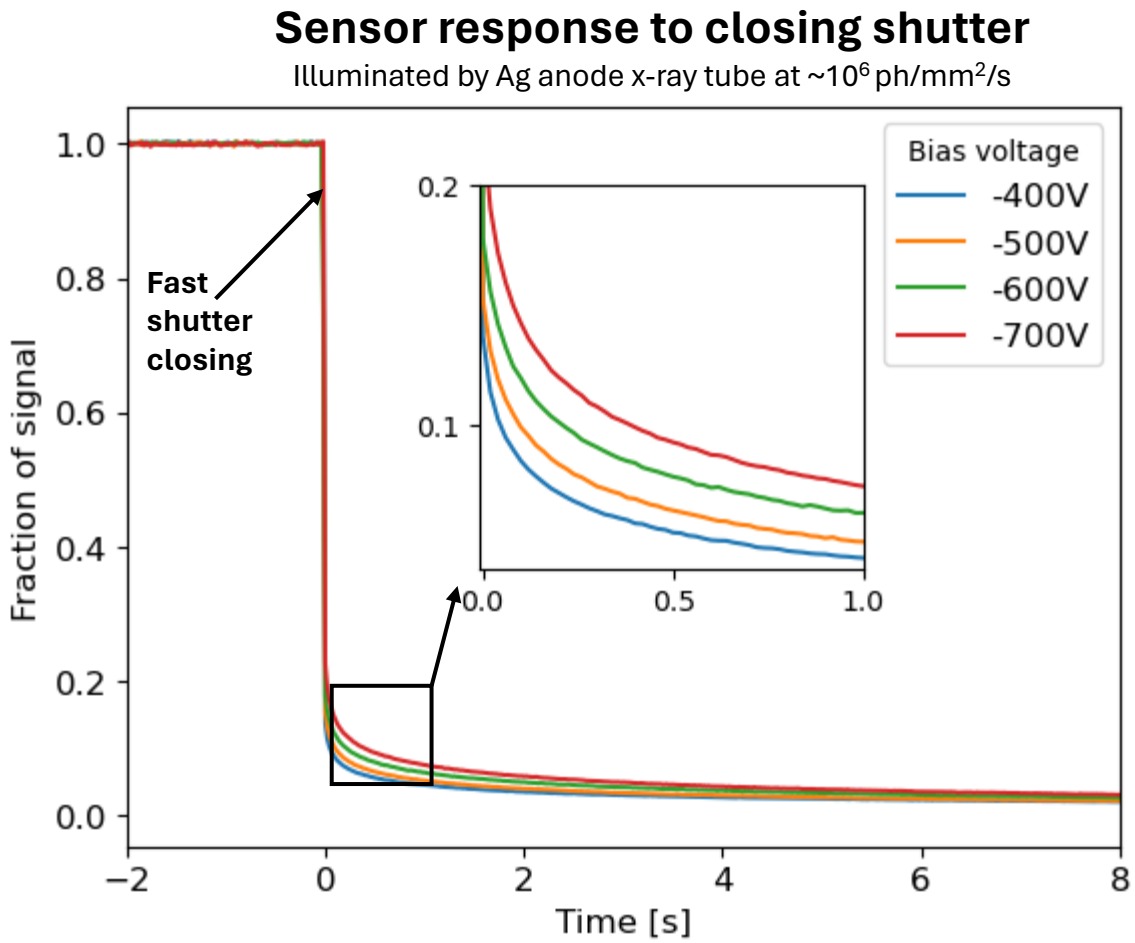

Is afterglow due primarily to bulk traps, surface traps, or a combination of both?

Afterglow vs Flux

- As traps fill, afterglow signal (relative to initial signal) decreases
- Promising for high flux (>10^7 ph/mm^2/s) applications

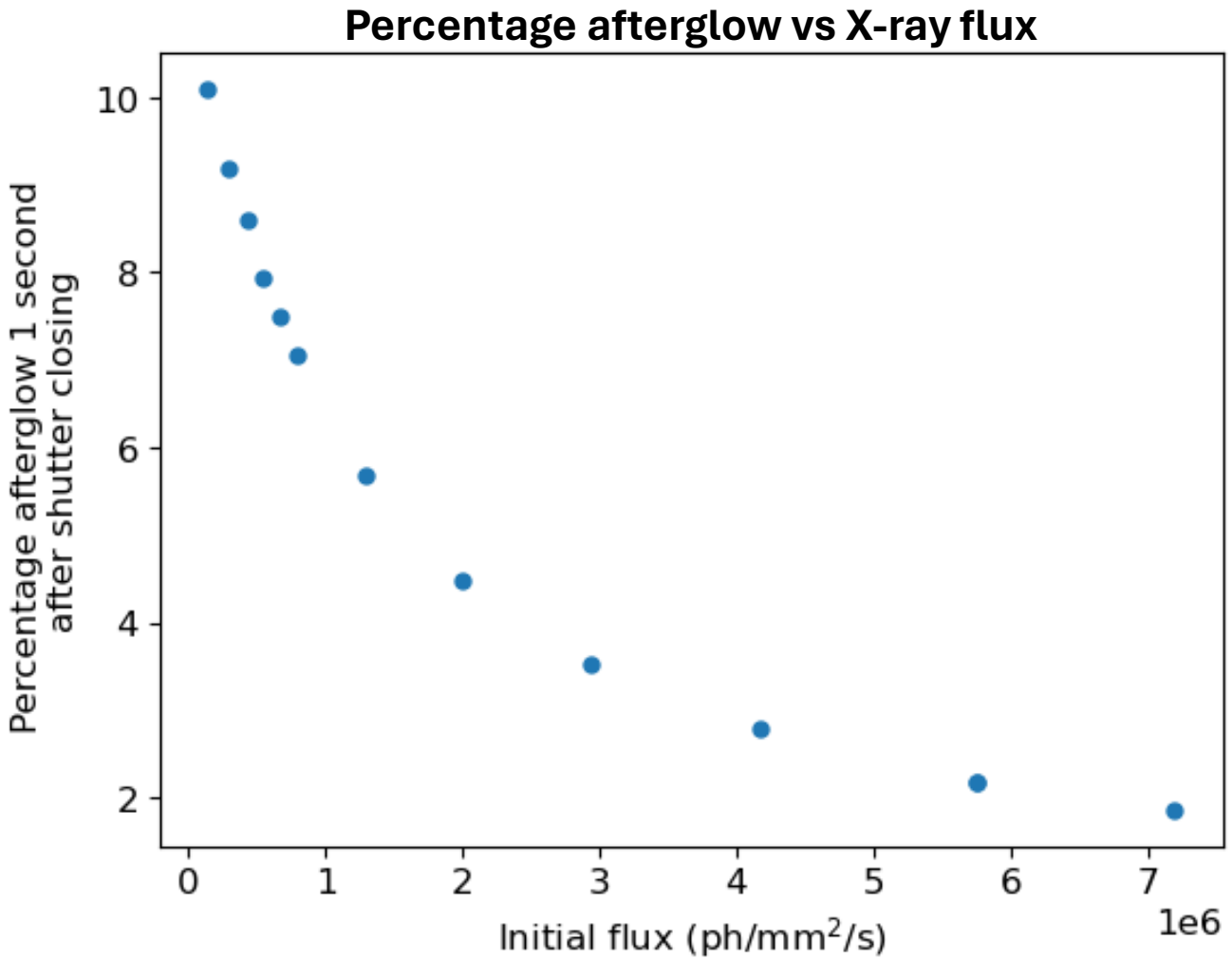

X-rays from Ag anode X-ray source, tube bias 40kV

Afterglow – electron vs hole collection

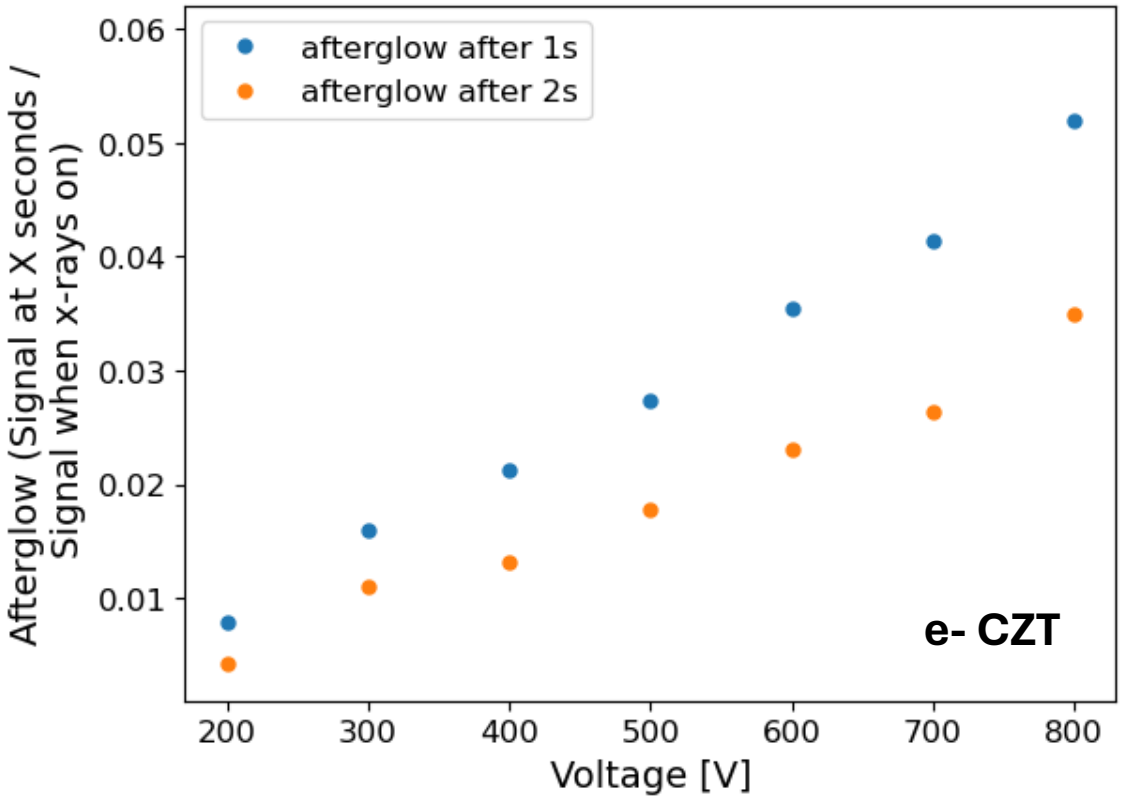

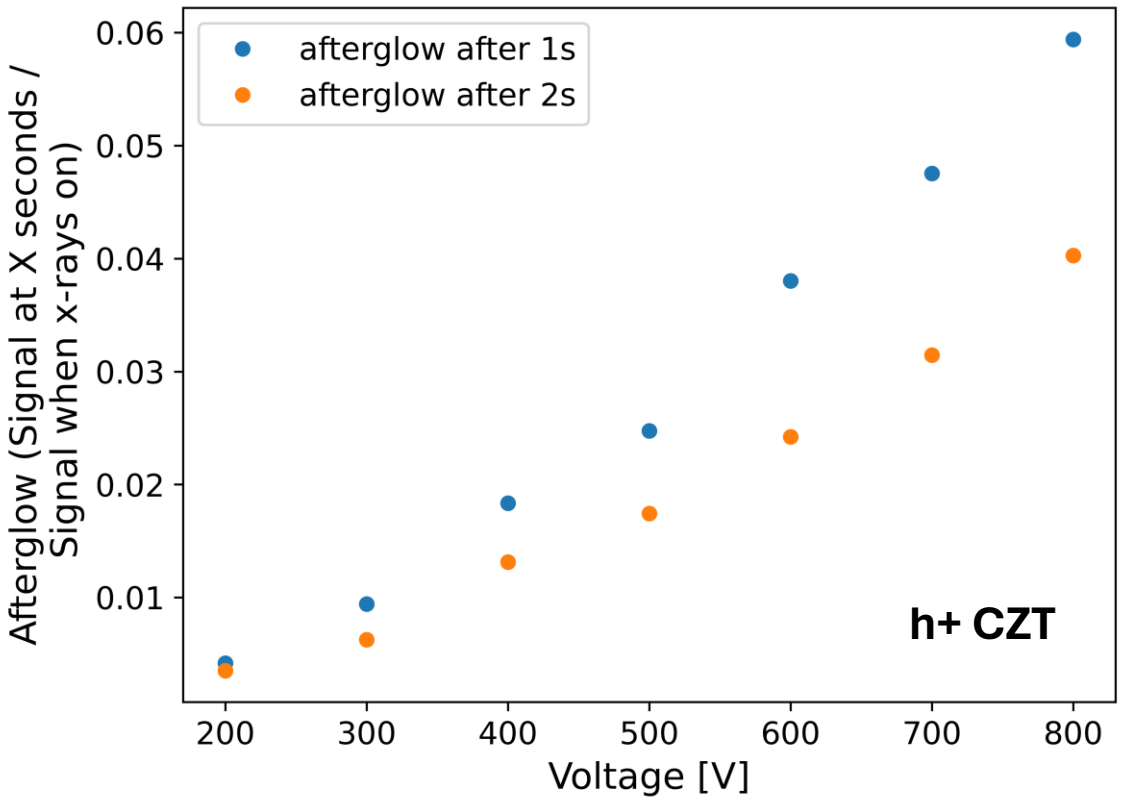

Electron and hole collecting sensors exhibit similar magnitude and duration of afterglow

Mitigating afterglow with LED illumination

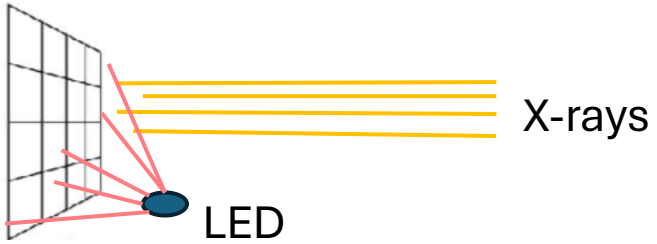

880 nm drop due to IR "Polarization"

- Can LED illumination of different wavelengths reveal the depth profile of afterglow-causing traps?
- Illuminated with 400 nm light (absorbed in top ~0.1 um) and 880 nm light (absorbed fairly uniformly)

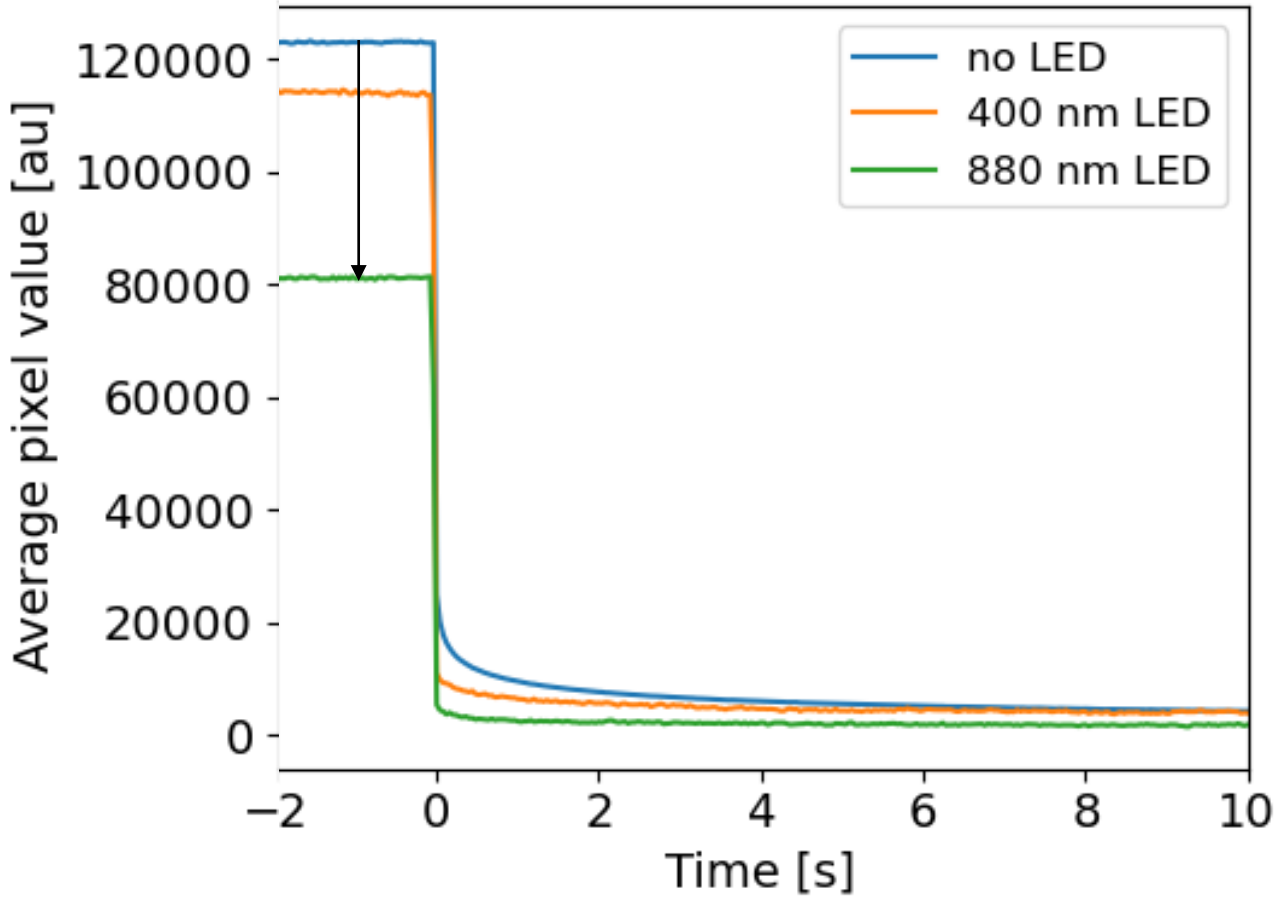

Conclusions

- High CCE above ~300 V in electron-collecting configuration
- Polarization resistance improved (compared to CdTe at same applied E-field), some changes observed when exposed to low-energy X-rays
- Significant afterglow on seconds timescale at low to moderate fluxes
  - Limits use for high-speed measurement at these fluxes

Thank you for your attention!

Support for detector development at Cornell has come from U.S. Department of Energy grants DEFG02-10ER46693, DE-SC0016035, DE-SC0004079, DE-SC0021026, and DE-SC0017631, as well as support from the NNSA to the mission of the Dynamic Compression Sector of the Advanced Photon Source at Argonne National Laboratory.

1. Gadkari, D., et al. "Characterization of 128× 128 MM-PAD-2.1 ASIC: a fast framing hard x-ray detector with high dynamic range." *Journal of Instrumentation* 17.03 (2022): P03003.
2. Philipp, H. T., Tate, M. W., Purohit, P., Shanks, K. S., Weiss, J. T. & Gruner, S. M. (2016). “High-speed X-ray imaging pixel array detector for synchrotron bunch isolation.” *J. Synchrotron Rad*. 23, (2015): 395-403.
3. Jiang, Yi, et al. "Electron ptychography of 2D materials to deep sub-ångström resolution." *Nature* 559.7714 (2018): 343-349.

Email:
laf233@cornell.edu

Backup material

MM-PAD Applications

Coherent diffractive imaging

PETRA-III / Mancuso (Eu-XFEL)

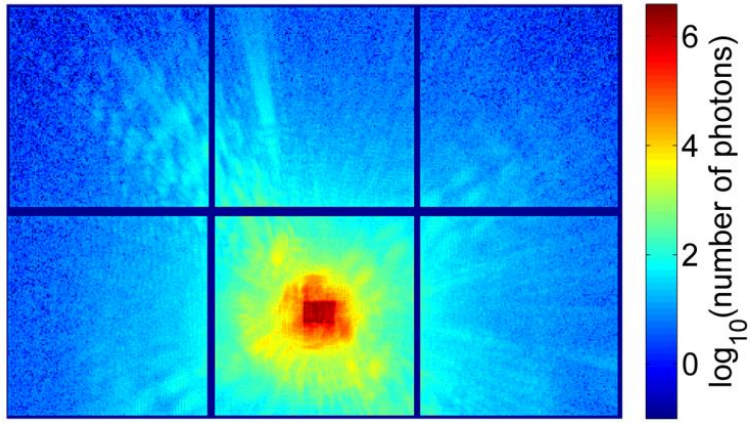

Giewekemeyer et al., *Journal of Synchrotron Radiation* (2014)

- Capture scattering pattern from Au test object, allowing ptychographic image reconstruction with ~25nm resolution
- **Key detector features:** wide dynamic range, fidelity at high incident photon rates (**>10⁷ ph/pix/s** in central spot)

Deformation in metals

CHESS / Beaudoin (U. Illinois)

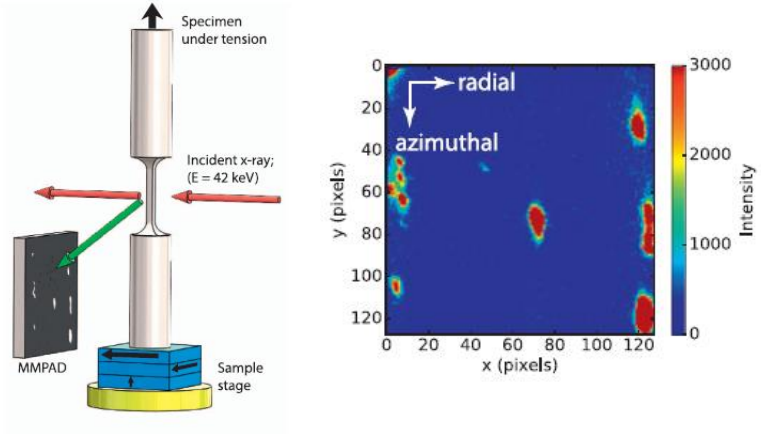

Chatterjee et al., *J. Mechanics & Physics of Solids* (2017)

- Probe grain-level deformation mechanisms and residual stress in polycrystalline Ti-7Al alloy under applied stress gradient
- **Key detector features:** CdTe sensor for efficient detection of 42 keV photons

Piezomagnetic ordering in UO2

APS / Gofryk (Idaho Nat'l Lab)

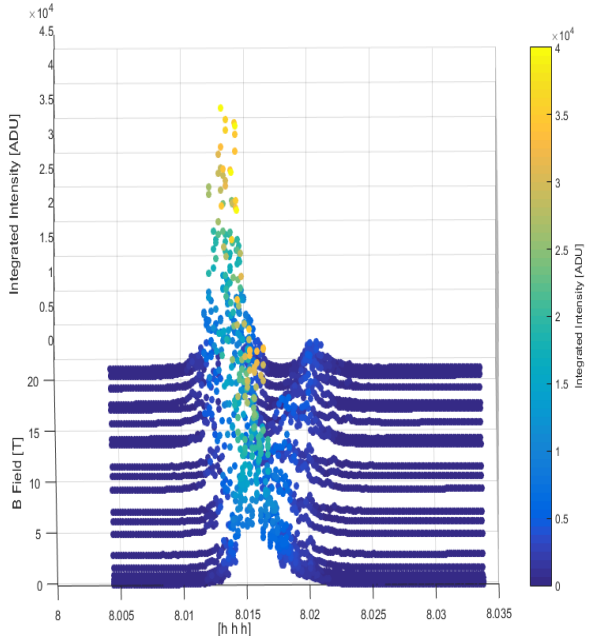

Antonio et al., *Nat. Communications Materials* (2021)

- Observe Bragg peak splitting in UO2 during 10ms magnetic pulse
- **Key detector features:** Fast (1 kHz) continuous frame rate